Use of a reciprocity technique to measure the radiation efficiency of a vibrating structure

Giacomo Squicciarini[1], Azma Putra[2]*, David J. Thompson[1], Xianying Zhang[1], Mohamed Azli Salim[2]*

[1] *Institute of Sound and Vibration Research, University of Southampton, Highfield, Southampton SO17 1BJ, United Kingdom*

[2] *Centre for Advanced Research on Energy, Faculty of Mechanical Engineering, Universiti Teknikal Malaysia Melaka (UTeM), Hang Tuah Jaya 76100 Durian Tunggal, Melaka, Malaysia*

Abstract

The reciprocity principle is well-known and has many applications in acoustics and vibro-acoustics. This paper discusses a reciprocity measurement method to determine the radiation efficiency of a vibrating structure. The method comprises two steps: (i) measurements of the acceleration response of the structure induced by a sound field in a reverberation chamber and (ii) measurements of the spatially-averaged squared transfer mobility of the structure. The approach is more flexible than a direct method and has the advantage that no shaker is required to excite the structure in the acoustic measurements. To demonstrate the applicability of this method, experiments were conducted on rectangular flat plates, on two components of a railway track test-rig and on three different built-up structures. For the plates and the railway rig components, comparisons are also made with theoretical models. It is shown that the measured results for each arrangement obtained using this reciprocity method provide good agreement with conventional direct measurements and with theoretical modelling. However, in most of the examples presented, the direct method has been found to be less practical and sometimes even less accurate than the reciprocal one, mostly due to the structure-shaker connection and to the inherent uncertainty of acoustic intensity measurements.

Keywords:
reciprocity, radiation efficiency, acoustics, vibro-acoustics, acoustic finite element, perfect matching layer, acoustic boundary element, plates, railway noise

1. Introduction

The radiation of sound from a vibrating structure can be defined in terms of its radiation efficiency, which is the sound power normalised by the surface area, the spatially-averaged surface velocity and the characteristic acoustic impedance of the medium. To measure this quantity two separate steps are required: in the first the acoustic power radiated by the vibrating body is measured, while in the second the spatially-averaged mean-square normal velocity is determined. Either the same excitation must be applied in each case, or the responses should be normalised in each case by the corresponding mean-square force amplitude.

A number of conventional methods are available that can be used to measure the radiated sound power. These include methods based on sound pressure measurements, viz. the free field method [1] or the reverberation room method [2], and the sound intensity method [3]. However, each of these 'direct' methods has limitations. For example, the results may be influenced by background noise, particularly those based on sound pressure measurements. Practical difficulties occur in cases where reflecting surfaces, or other obstacles, are located close to the source which

*Corresponding author. Tel.:+60 6 234 6720; fax:+60 6 234 6884.
Email address: azma.putra@utem.edu.my (Azma Putra[2])

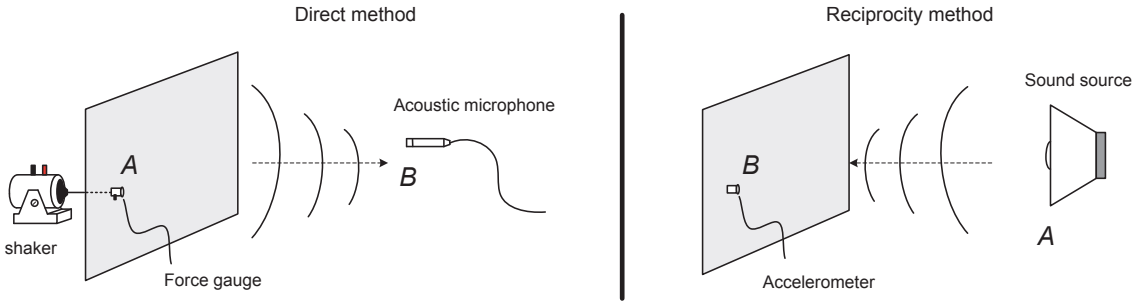

Figure 1: Illustration of direct and reciprocity techniques. *A*: Exciter location, *B*: Response location.

may prevent access to the required measurement or excitation points. Where the response to a known force is required, the device used to excite the structure, usually a shaker, may affect the structural behaviour and may also radiate noise which can complicate acoustic measurements. Moreover, the effectiveness of force transmission from the shaker to the structure decreases with increasing frequency, especially when a stinger is used. Good discussions on shaker-stinger-structure coupling effects can be found for example in [4] and [5]. In order to overcome these limitations, a 'reciprocal' technique can be applied; in the proposed method the structure under test is excited by sound in a reverberation chamber and the consequent vibration response is measured, for example using accelerometers.

The idea of using reciprocity for acoustics was proposed by Lord Rayleigh [6] who stated that the acoustic pressure produced at a point *A* in a fluid by a simple harmonic, omni-directional, point-source having a certain volume velocity and located at another point *B* in the fluid is the same as the pressure that would be produced at *B* by the same source located at point *A* [7]. This applies irrespective of the presence of arbitrary boundaries to the fluid. The principle of reciprocity can also be applied to structural response, where the force and response positions on a structure can be exchanged.

The principle of acoustic reciprocity was extended by Lyamshev [8][9] to the case of the vibro-acoustic behaviour of an elastic structure, as illustrated in Figure 1. He demonstrated a relationship between the acoustic pressure at a point *B* due to a vibrating structure subjected to a harmonic mechanical force at a point *A* and its reciprocal situation: that is, in the absence of the mechanical force, the vibration velocity that is produced at the point *A* on the structure due to an acoustic excitation by a point source located in the fluid at the point *B*.

Fahy presented review papers in 1995 [10], and in later in 2003 [11], in which, along with a historical description of the reciprocity principle in vibro-acoustics, several applications are discussed. In contrast to the method outlined in this work, in most of the cases discussed by Fahy the methods do not rely on the use of a reverberation chamber. These papers represent a comprehensive overview of reciprocity in vibro-acoustics and give good background for the method proposed here. An interesting method, named the 'monopole array model', is discussed which consists of an application of reciprocity to the noise radiated from vibrating surfaces. It is based on subdividing the radiating surface into small areas radiating as correlated or uncorrelated monopoles and in an experimental characterisation of the monopole properties through reciprocity. The extension of the reciprocity principle to include the vibrating structure, as demonstrated by Lyamshev, is also discussed in [10] and further applications are detailed by Verheij in [12] and [13]. In the examples summarised in the above-mentioned papers it is also shown how reciprocity can be of support in developing and applying inverse force identification techniques. In these cases the transfer function between sound pressure at a receiver location and force applied to a structure can be alternatively obtained by placing an omnidirectional source with known volume velocity at the receiver position and by measuring the free velocity thus generated on the structure in the same position and direction as the original excitation force. A similar principle is envisaged in this work although the presence of a reverberant room relaxes the requirements necessary on the source.

The reciprocity principle with 'monopole array model' was applied by Zheng et al. [14] to measure the sound pressure radiated by an internal combustion engine. The engine surface was divided into discrete sub-areas and it was shown that the mean-square pressure at the receiver point could be found from the sound power of each sub-area and the acoustic transfer function between the surface pressure on the engine and the volume velocity of a monopole source. The sound intensity scanning method was employed to measure the sound power of the operating engine and the acoustic transfer function was measured reciprocally between the source strength of a monopole source and the

sound pressure measured with a microphone located close to the non-operating engine.

Application of Lyamshev reciprocity has led to various uses in vibro-acoustic problems. It has been adopted for example in studying tyre induced vehicle interior noise, [15] [16]. Mason and Fahy [17] proposed this technique to measure the transfer function between a point force acting on the exterior of an aircraft fuselage and the sound pressure generated inside the cabin. As the fuselage is a non-uniform structure, a procedure was devised whereby the fuselage is discretised into a number of segments and where the transfer function from the internal volume velocity due to a monopole source and the resulting surface vibration volume velocity on each discrete segment need to be measured. This approach was first validated using a clamped plate on the top of a box excited by a point source from the inside. This technique was then applied by MacMartin et al. [18] to a real aircraft fuselage. Comparison with the direct method was also presented with very good agreement.

In general, Fahy [10] also reports that reciprocal techniques have often been found to be cheaper, less time-consuming, more convenient and sometimes also more accurate than the equivalent direct measurements. However, in terms of characterising sound sources and measuring sound power from operating machinery, international standards are focussed on direct techniques such as the free field method [1], the reverberation room method [2] and the sound intensity method [3]. Other important established direct techniques to measure the acoustic intensity vector field, and therefore to quantify acoustic power, are the Nearfield Acoustic Holography (NAH) [19] and its extension to sound radiated in an enclosed environment, named Phonoscopy [20]. These techniques are largely employed in applications aimed at localising noise sources and they can provide a high degree of accuracy. However, they rely on a large number of sensors and this limits their usage for affordability reasons.

Crocker and Price [21] have shown that Statistical Energy Analysis (SEA) can be successfully used in determining the vibroacoustic properties of panels. In particular they have shown comparisons between SEA predictions and measurements performed on a panel in a reverberant room and in between two adjacent rooms to measure the radiation resistance and transmission loss of the panel. To measure these quantities a direct technique was adopted while other SEA parameters, such as coupling factors and modal densities, were measured using reciprocity. This technique has also been applied to ribbed panels [22] and to foam-filled honeycomb sandwich panels showing satisfactory results of radiation resistance compared with predicted formulae [23].

This paper focuses on the measurement of the radiation efficiency and radiated sound power of a vibrating structure using a reciprocity technique. In particular, the Lyamshev technique is extended to include measurements in a reverberation chamber. Only the case of mechanical excitation is considered, although it is recognised that the radiation efficiency due to acoustic excitation is sometimes of interest. After presenting the theory and the methodology adopted (Sections 2 and 3) attention is focused on several examples to illustrate the applicability of the method. Firstly a simple rectangular plate with free edges is considered with two different thicknesses. The results are compared with measurements made using a conventional direct approach in which the power is measured using an intensity probe as well as with the results of corresponding theoretical models developed by means of acoustic finite element modelling. Attention is then focused on two separate components of a scale model of railway track test-rig being developed at the Institute of Sound and Vibration Research (see [24] for more details). For both a rail and a sleeper the radiation efficiency is measured using both the reciprocity method and a direct method using an intensity probe. Measurements are also compared with predictions obtained using a boundary element model. Finally three, more complex built-up structures are considered. They consist of closed steel box structures made of steel plates welded together. In this case the radiated sound power normalised by the input force was measured using both the reciprocity and direct techniques, both of which were applied in a reverberation chamber. Section 2 describes the measurements required to determine the radiation efficiency. Section 3 introduces the background theory of reciprocity and its application to the current method. The experiments, and their theoretical counterparts, are described in Section 4 for the plates, Section 5 for the scale rail and sleeper and Section 6 for the built-up structures.

2. Methods for measuring radiation efficiency

This section introduces the measurement of the radiation efficiency, or radiation ratio, of a vibrating structure. This is a dimensionless quantity that indicates how much sound power W a given structure radiates compared with an ideal case of a piston of the same surface area radiating plane waves and vibrating with a mean-square velocity equal to the spatially-averaged mean-square velocity of the structure. This can be written as [7]

$$\sigma = \frac{W}{\rho c S \left\langle \overline{v^2} \right\rangle} \tag{1}$$

where ρ is the air density, c is the speed of sound, S is the surface area of the structure and $\left\langle \overline{v^2} \right\rangle$ is its spatially-averaged mean-square vibration velocity normal to the surface. The quantities σ, W and $\left\langle \overline{v^2} \right\rangle$ are functions of frequency and are commonly expressed in frequency bands such as one-third octaves. Normalising by the mean-square force acting on the structure in the frequency band, Eq. (1) can be expressed as

$$\sigma = \frac{W/\overline{F^2}}{\rho c S \left\langle |Y_t|^2 \right\rangle} \tag{2}$$

where $\left\langle |Y_t|^2 \right\rangle = \left\langle \overline{v^2} \right\rangle / \overline{F^2}$ is the spatially-averaged squared transfer mobility.

From Eq. (1) it can be seen that, to determine the radiation efficiency, two measurements are required: an acoustic measurement, namely the radiated sound power, and a mechanical measurement, namely the spatially-averaged squared velocity. These must be measured for the same excitation conditions. Alternatively, using Eq. (2), the measurements to be made consist of the sound power per unit mean-square force and the spatially-averaged mobility. In most of the cases to measure the mobility the structure under study is excited by a known force input, either using an electrodynamic shaker and force transducer or an instrumented hammer, and the acceleration (or velocity) at different points across its surface is measured. For the acoustic measurement, various direct methods are available to measure the radiated sound power, or alternatively reciprocity techniques can also be used, in which the structure is excited by acoustic excitation from an external sound source and the resulting vibration of the structure induced by the incident sound is measured, see Figure 1.

In the case of the direct methods, if the mechanical excitation uses an electrodynamic shaker particular attention has to be paid to the way in which the shaker and structure are connected and to the noise radiated by the shaker itself as this may contaminate the measured sound. There are, in fact, difficulties in exciting a structure with an electromechanical shaker, in particular at higher frequencies. Mass loading may occur due to the force transducer and its mounting arrangement, a stinger should be used to connect the shaker to the structure to avoid moment excitation. This has to be as straight as possible to avoid misalignment and to obtain the correct transmission of force. Finally dynamic coupling between the shaker and the structure may occur, affecting the force spectrum. Some of these aspects will be illustrated in the results shown below.

For the acoustic measurements, noise from the shaker is a particularly important issue for structures that have a low sound radiation. Although sound intensity measurements can be used to minimise the effect of such extraneous noise sources, it may nevertheless be necessary to shield the noise from the shaker, e.g. using an enclosure. A problem also arises for certain experimental arrangements where it is difficult to install an exciter due to access problems.

Reciprocity methods have less constraints: in the absence of the shaker, the structure can be conveniently arranged as in its practical installation, including locations close to reflecting surfaces. It is also often much more convenient and easy to install a sound source than a shaker. Nevertheless, for the reciprocity method the measurement of the vibration response of the structure to the acoustic excitation may be subject to errors. For example, a structure with a low response requires a sensitive sensor to measure its low vibration levels with sufficient accuracy and, moreover, care is required not to load the structure with the mass of the transducer. The transducer should not be sensitive to acoustic excitation.

The particular technique proposed in this paper involves the use of a reverberation chamber for the reciprocal acoustic measurement, which obviously implies that the structure to be tested has to be portable to allow it to be moved into the testing room. The next section discusses the governing equations for the reciprocity method used to measure the radiation efficiency under these conditions.

3. Application of reciprocity principle to the measurement of radiation efficiency in a reverberant field

Lyamshev [8] showed that the transfer function between a point force F exciting a linear elastic structure at a point A and the resulting sound pressure p at a particular observation point B is identical to the transfer function between a

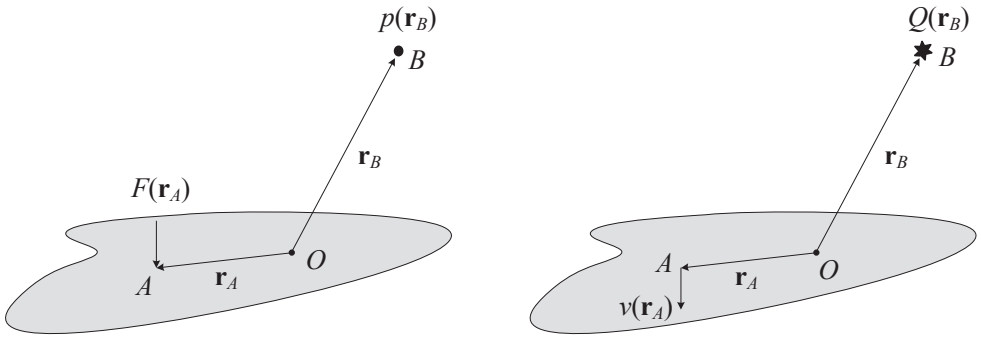

Figure 2: Basic concept of reciprocal measurement of sound radiated by an elastic structure excited by a point force. (a) Direct measurement, (b) reciprocal measurement.

volume velocity Q of a point monopole located at the former observation point B and the resulting vibration velocity v produced at the former excitation point A, in the same direction as the excitation force. This is shown schematically in Figure 2. Hence

$$\frac{p(\mathbf{r}_B)}{F(\mathbf{r}_A)} \equiv -\frac{v(\mathbf{r}_A)}{Q(\mathbf{r}_B)} \tag{3}$$

where $\mathbf{r}_A$ and $\mathbf{r}_B$ are the position vectors of the point on the structure and of the point in the fluid, respectively and all quantities are complex functions of frequency.

Consider next an experiment conducted in a reverberant field. The sound power W_{rad} radiated by a vibrating structure in the direct experiment in Figure 2(a) in a given frequency band can be normalised by the mean-square force $\overline{F_A^2}$ exciting the structure at the point A to give [25]

$$\frac{W_{rad}}{\overline{F_A}^2} = \frac{S\bar{\alpha}}{4\rho c}\frac{\left\langle \overline{p^2} \right\rangle}{\overline{F_A}^2} \tag{4}$$

where $S\bar{\alpha}$ is the room absorption and $\left\langle \overline{p^2} \right\rangle$ is the spatially-averaged mean-square sound pressure in the room caused by the vibrating structure. In a reverberant field the sound pressure is approximately the same at any observation point B in the room. Therefore, to simplify the notation, Eq. (4) can be approximated in terms of the mean-square pressure at an arbitrary position B:

$$\frac{W_{rad}}{\overline{F_A^2}} = \frac{S\bar{\alpha}}{4\rho c}\left(\frac{\overline{p_B^2}}{\overline{F_A^2}}\right) \tag{5}$$

Using the principle of reciprocity from Eq. (3), Eq. (5) can then be written as

$$\frac{W_{rad}}{\overline{F_A^2}} = \frac{S\bar{\alpha}}{4\rho c}\left(\frac{\overline{v_Q^2}}{\overline{Q^2}}\right) \tag{6}$$

where $\overline{v_Q^2}$ is the mean-square velocity of the plate at the point A due to the acoustic excitation from a monopole source having mean-square volume velocity $\overline{Q^2}$ at the point B.

The source volume velocity Q in the reciprocal measurement can itself be determined from a sound power measurement. The radiated sound power W_Q of a compact source is given by [26]

$$W_Q = \rho c \overline{Q^2}\frac{k^2}{4\pi} \tag{7}$$

where $k = \omega/c$ is the acoustic wavenumber and ω is the circular frequency. The sound power W_Q can be obtained by measuring the spatially-averaged mean-square pressure $\left\langle \overline{p_Q^2} \right\rangle$ in the reverberant room induced by the source Q. As in Eq. (4) this is given by

$$W_Q = \frac{S\,\bar{\alpha}}{4\rho c} \left\langle \overline{p_Q^2} \right\rangle \tag{8}$$

After re-arranging Eq. (7) and Eq. (8), the mean-square volume velocity $\overline{Q^2}$ is given by

$$\overline{Q^2} = \frac{S\,\bar{\alpha}\pi}{\rho^2\omega^2} \left\langle \overline{p_Q^2} \right\rangle \tag{9}$$

since $k = \omega/c$. Hence, substituting this into Eq. (6) gives

$$\frac{W_{rad}}{\overline{F^2}} = \frac{\overline{a_Q^2}}{\left\langle \overline{p_Q^2} \right\rangle} \left(\frac{\rho}{4\pi c} \right) \tag{10}$$

where $a_Q = j\omega v_Q$ is the acceleration response of the structure and $\left\langle \overline{p_Q^2} \right\rangle$ is the spatially-averaged mean-square acoustic pressure developed in the room due to the sound source. The acceleration could also be averaged over different source positions in the room, equivalent to the averaging of squared pressure in Eq. (4). The radiation efficiency of the vibrating structure is finally obtained by using Eq. (10) together with the spatially-averaged transfer mobility $\left\langle |Y_t|^2 \right\rangle$ for a force at A in Eq. (2).

It may be noted that there is no requirement to measure the reverberation time, or absorption, of the reverberation chamber as this cancels in the equations; the requirement is only that the field is reverberant. There is also no need to have a compact monopole source as long as the diffuse field is excited; the source positions are also unimportant.

4. Freely suspended plate

The measurement of radiation efficiency using the proposed reciprocity technique is presented first for simple rectangular plates with free edges. For comparison, a conventional measurement using a direct method is also discussed and an acoustic finite element model is shown for reference purposes. The advantages and disadvantages of the two measurement methods are addressed.

The experiments have been conducted using two rectangular aluminium plates with dimensions 0.4 m $\times$ 0.3 m. Their thicknesses were 1.5 mm and 3 mm, giving critical frequencies of 8 kHz and 4 kHz, respectively. Patches of damping material have been attached to the plates to increase their damping so as to make the plates more representative of an engineering structure.

To illustrate the measurements described in the next sections Figure 3(a) shows the plate excited by a shaker and being scanned with a two-microphone intensity probe while the set up for reciprocal measurements in the reverberant room is shown in Figure 3(b).

4.1. Measurements of plate vibration

In order to estimate the radiation efficiency of a vibrating structure it is necessary to measure the velocity of the vibrating surfaces. Two different techniques have been tested in the present work and it will be shown that one is more appropriate together with the direct measurements of sound power while the other is more suitable for the reciprocal method.

The plate average mobility has first been measured using impact excitation. A PCB instrumented hammer type 086D80 has been used to strike the plate at 43 locations on its surface; the striking points are shown in Figure 4. On the other side of the plate, at the position A shown with an asterisk, a PCB miniature accelerometer type 352C22 (with a mass of 0.5 g) was attached to measure the acceleration. The squared magnitude of the 43 measured mobilities has then been averaged for use as $\left\langle |Y_t|^2 \right\rangle$ in Eq (2). Note that, for convenience, these measurements have also used reciprocity: the position A has been used as the response point rather than the forcing point.

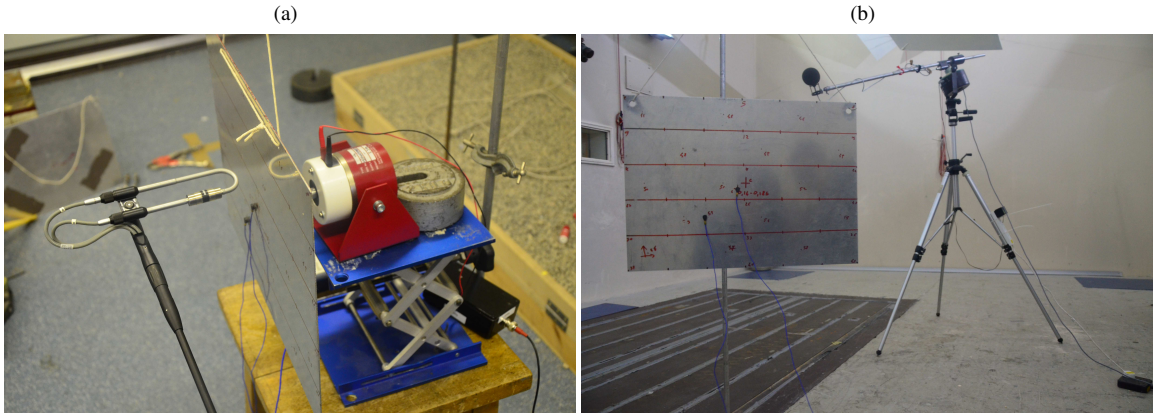

Figure 3: (a) Direct measurement of sound intensity with two-microphone intensity probe. (b) Arrangement of the plate in the reverberant room, microphone boom is visible in the background.

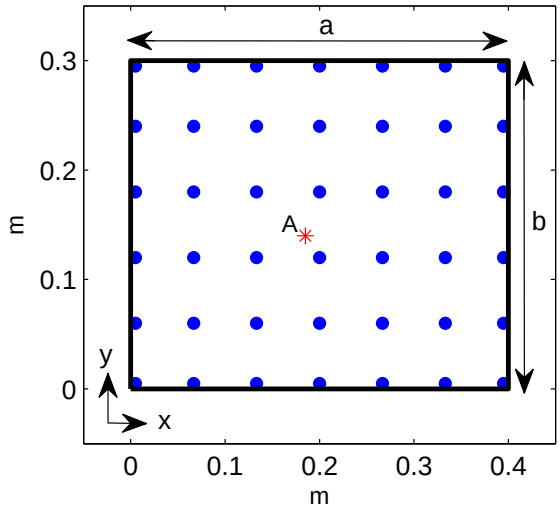

Figure 4: Measurement grid adopted for mobility measurement on the plates; •: measurements point for transfer mobility; ∗: driving point location, A.

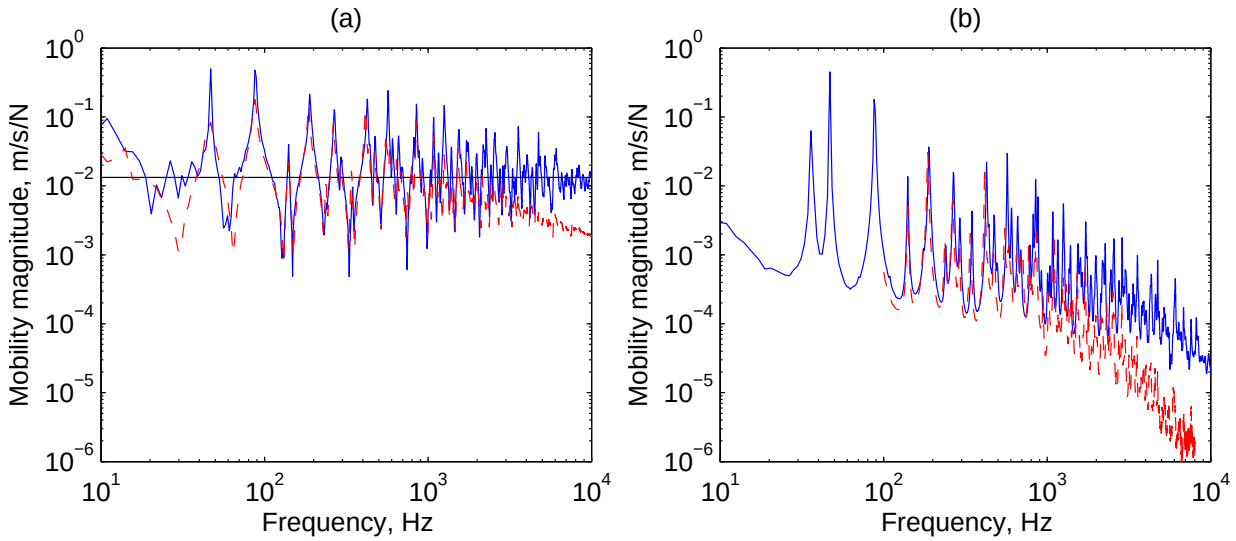

Figure 5: Driving point mobility (a) and average mobility (b) measured with impact hammer technique (—) and with shaker excitation (- - -). Continuous horizontal line in (a) represents the mobility of an infinite aluminium plate of thickness 1.5 mm.

Even on a homogeneous structure the choice of the position and number of measuring points is important. The grid adopted here consists of 7×6 points plus the forcing point, the latter being located at 15 mm from the plate centre in the x direction and 10 mm in the y direction. The effect of the number of measurement points is briefly discussed in Appendix A where it is shown that, in order to avoid unwanted variability among the three methods discussed below, the measurement grid has to be kept the same.

As an alternative to hammer excitation, an electrodynamic shaker (Data Physics type V4) has been used to excite the plate via a 25 mm long stinger and the force was measured with a force gauge (PCB type 288D01 having a mass of 19.2 g) attached to the plate. The plate velocity has been measured over the same grid of 43 points shown in Figure 4 using a Polytec scanning laser vibrometer, type PSV 300, to obtain the transfer mobilities which have been averaged over all the points. Again this quantity can be adopted in Eq. (2). In this case the product of the mean-square measured force and the average mobility gives the spatially-averaged mean-square velocity of the plate, $\left\langle \overline{v^2} \right\rangle$, which can be introduced into Eq. (1) when the acoustic power of the vibrating structure is known. Alternatively the spatially-averaged mean-square velocity can be directly measured with the laser scanner thus avoiding the use of a force gauge, but in this case the level of excitation of the plate must be kept the same when measuring velocity and when measuring acoustic power.

As an example, Figure 5 compares the driving point mobility (a) and average mobility, $\left\langle |Y_t|^2 \right\rangle$ (b), of the 1.5 mm plate measured with the two different methods. The driving point mobility is also compared with the mobility of an infinite plate. The driving point mobility of a finite plate should tend, at high frequency and on average, to the mobility of the infinite plate [27]. This is the case for the mobility measured with the hammer and accelerometer but there is clearly a mass-loading effect in the case of the measurement performed with the shaker due to the force transducer. Moreover, both Figures 5(a) and 5(b) show that the coupling with the shaker has also added some apparent damping to the plate seen as a reduction in amplitude of the peaks. This is actually caused by the force spectrum in the coupled system and will be discussed in Section 4.6 below. On the 3 mm plate (not shown) the mass-loading effect has been found to be almost absent but the apparent damping has still been increased.

A further check for the effect of the plate-shaker coupling can be performed by comparing the average mobility $\left\langle |Y_t|^2 \right\rangle$ with the mean-square average velocity $\left\langle \overline{v^2} \right\rangle$, the former measured with the hammer and accelerometer and the latter with the shaker and laser vibrometer. They are shown in Figure 6 for both the plates tested. The average velocity has peaks at slightly different frequencies than the average mobility and the apparent damping is increased; the amplitude of the peaks can be seen to be smaller for the average velocity. The reason for the shift of velocity

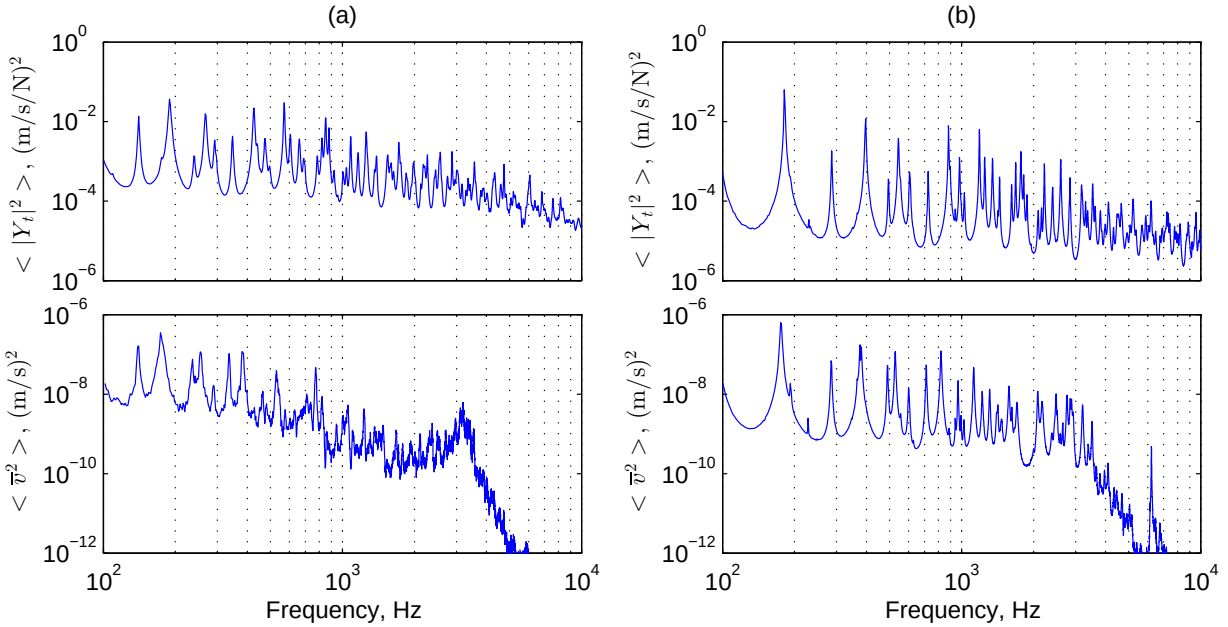

Figure 6: Average mobility $\left\langle |Y_t|^2 \right\rangle$ measured with impact hammer and average velocity $\left\langle \overline{v^2} \right\rangle$ measured with shaker. (a) 1.5 mm plate; (b) 3 mm plate.

maxima compared to the mobility is again caused by the force spectrum. This is an important outcome to consider when normalising the acoustic power to the average vibration of the plate. If the presence of the shaker and stinger influence the vibrational behaviour of the structure, as in these cases, the average velocity (or average mobility) to be used in Eq (1) (or in Eq (2)) must be the one measured with the same forcing condition adopted to measure the sound power. It is then expected that the two techniques cannot be in full agreement with one another, as will be shown later.

Figure 6 also shows that average velocity rolls off starting from about 3 kHz. Again this is a consequence of the force spectrum that shows the same trend. It has been found that the force starts to roll off at the first bending natural frequency of the stinger. Several attempts have been made in trying to improve the force transmission without any noticeable benefit with respect to the results shown in Figure 6.

4.2. Direct acoustic measurements

In the case of direct acoustic measurements the sound power has been measured using the sound intensity technique by scanning the front face of the plate with the centre of the probe located at approximately 5 cm from the plate surface, see Figure 3(a). The intensity probe was a B&K type 3599 two-microphone probe with a 8.5 mm spacer giving a valid measurement range between 250 Hz and 6 kHz. Signal conditioning and post-processing have been performed through a B&K Pulse system type 3560c and the sound intensity has been recorded in one-third octave bands and exported for use in calculating the sound power. This has been obtained by adding up the product of the sound intensity normal to the surface and the associated area of the plate as

$$W = \sum_{i=1}^{n_S} I_{ni} S_i \tag{11}$$

where the summation is intended over all the n_S scanned surfaces while I_{ni} represents the time averaged intensity normal the the i-th surface S_i. Note that in this case only one surface has been scanned, assuming that the power radiated by the two sides is the same, but in other applications described below a full virtual enclosure is defined

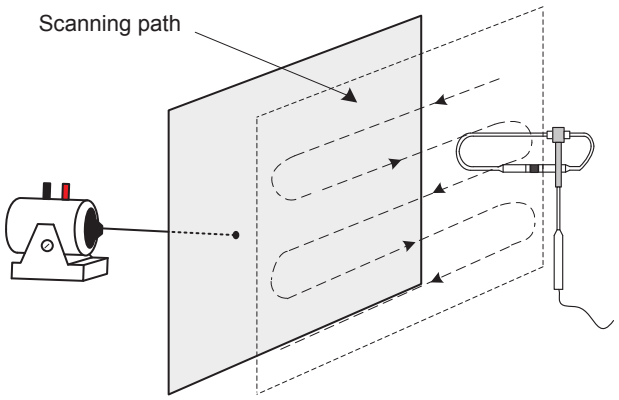

Figure 7: Measurement setup for the sound power measurement using the direct method.

around the vibrating structure and the summation extends over six faces. A graphical representation of the procedure is shown in Figure 7.

The radiation efficiency of the plate has been calculated by directly applying Eq. (1), with the mean-square velocity obtained by exciting the plate with the shaker and measuring the velocity with the laser vibrometer. Before applying Eq. (1) the mean-square velocity spectrum has been converted into one-third octave bands for consistency with the measured acoustic power.

Another similar alternative has been also tested to measure the radiated power of the plate. It consists in using the intensity probe in accordance with the procedure given in ISO 9614-3:2002 [3]. For this purpose, a closed virtual box has to be defined in order to visualise the areas to be scanned with the intensity probe. The boundaries of this box have been demarcated with tiny wires. To minimise the influence of noise radiated by the shaker this was placed outside the virtual box and a foam sheet was located in front of it. A long stinger (150 mm) has been adopted to allow enough space between the shaker and the plate for the scanning probe to fit between them. However the noise produced by the shaker compared with the noise radiated by the plate has been found to be negligible. The long stinger makes the force transmission less efficient and the scanning procedure becomes longer and more difficult as the likelihood of touching the plate or the shaker with the scanning probe increases. With the equipment available it has been found that adopting the long stinger makes the transmitted force roll off starting from 1 kHz while with the shorter stinger the force starts decreasing at about 3.5 kHz. For these reasons, the procedure of scanning over a closed volume has been discarded for this application and the acoustic intensity has been measured over one face of the plate only. Other smaller equipment for measuring sound intensity could be adopted with greater ease when scanning over a closed volume.

4.3. Reciprocity measurements of sound power

To measure the sound power radiated by the plate using the reciprocity technique, the experiment was conducted in a reverberation chamber at the ISVR having a volume V of 348 m^3 and a surface area of 302 m^2. Reverberation times of the empty room are reported in Table 1. Note that these are shown for reference purposes only and with the aim of characterising the reverberant room used in the experiments but they are not required in the methodology adopted here to measure the radiation efficiency. The room is constructed with non-parallel walls to give a good diffuse field and the internal surfaces are finished with a hard gloss paint to give a high reflection coefficient. Diffusing panels are fitted.

By applying the equation for the Schroeder frequency ($f_S = 2000(T_{60}/V)^{1/2}$) [28] it can be found that the first frequency band above which a diffuse field can be assumed is centred at 315 Hz. Nevertheless, results are presented here starting from 100 Hz.

To measure the plate response, a miniature accelerometer was attached to the plate surface at the same location A used when measuring the plate mobility with impact excitation and where the shaker was attached in the direct method (see Figure 4). The measurement covered the range up to the 8 kHz one-third octave band. It is important

Table 1: Reverberation time of the large reverberation chamber at the Institute of Sound and Vibration Research.

Centre Frequency (Hz)	100	125	160	200	250	315	400	500	630	800	1k
Rev. time T_{60}, s	8.8	11.1	9.7	11.7	11.6	9.4	8.7	7.5	7.0	6.4	6.1

1.25k	1.6k	2k	2.5k	3.15k	4k	5k
6.0	5.7	5.2	4.6	3.9	3.2	2.5

that the accelerometer itself should not be sensitive to the acoustic excitation. Besides its light weight to avoid mass loading to the plate, use of the miniature accelerometer here should also be beneficial in minimising this effect.

Figure 8 shows the measurement setup in the experiment, see also Figure 3(b). The plate under test has been located vertically at three locations in turn in the room, each about 2 m from the wall and more than 1 m from the floor. The room has been fed with random broadband noise up to 10 kHz. A B&K pressure microphone type 40AG was installed on a rotating microphone boom to obtain the spatially-averaged sound pressure in the room. The signal processing was carried out using a Data Physics analyser, type DP240. It is important in this reciprocal measurement to have sufficient sound energy to excite the structure under test.

Figure 9 plots the average sound pressure level (SPL) spectrum in one-third octave bands during acoustic excitation of the room as well as the noise floor in the room (i.e. measured when the loudspeaker was switched off). The SPL falls below 63 Hz, but above this frequency up to 5 kHz the spectrum is almost flat with an average one-third octave band level of 87 dB; it slowly decreases at higher frequency due to limitations of the loudspeakers used. The background noise can be considered negligible.

Figure 10(a) shows the measured mean-square acceleration spectrum compared with the noise floor of the accelerometer. At frequencies below 100 Hz the acceleration spectrum has a similar level to that of the noise floor. This is due to the small values of radiation efficiency for the flat plate at low frequencies.

The measured normalised sound power, $W/\overline{F^2}$ is shown in Figure 10(b). The increasing trend of the sound power with frequency approaching the critical frequency (expected at 8 kHz for the 1.5 mm plate and 4 kHz for 3 mm plate) can be observed. The sound power shown is the result of averaging results obtained with three different positions of the plate in the chamber. The difference among the three plate positions has been found to be small, the three lines falling in a corridor with an average width of about 1.5 dB, which demonstrates that a good diffuse field is developed in the reverberant chamber.

4.4. Finite element modelling

An acoustic finite element model of the two plates has also been developed in order to provide a reference for the two types of measurement. A commercial software (COMSOL Multiphysics) has been adopted. The plate has been modelled with thin shell elements with full coupling with the surrounding air through a module called 'Acoustic-shell interaction' in the software. The plate has been located in a spherical air domain bounded by a layer of absorbing elements to mimic the boundary conditions at infinity, the so-called Perfectly Matched Layer (PML), see e.g. [29] and [30]. A constant loss factor is assigned to the plate; its value has been chosen to give a good fit with the spatially-averaged mobility as measured with impact hammer on the freely suspended plate. This resulted in a loss factor of 0.0085 for the 3 mm thick plate and 0.012 for the 1.5 mm one. The measured damping of the 1.5 mm plate actually shows a stronger frequency dependence but for simplicity this has not been included in the numerical model. To optimise the computational time the frequency range spanned in the calculation has been divided into four parts and the size of the element mesh has been set in order to follow the rule of at least five elements per acoustic wavelength, in the air domain, and at least five elements per structural wavelengths over the plate. Element order has been set to be quadratic. The acoustic power due to a unit force has been calculated by integrating the intensity over the plate surface. The power has then been normalised by the spatially-averaged mean-square velocity to obtain the radiation efficiency, as in Eq. (1). The input force has been located at the same position A at which the input force was given in the direct method and at which the accelerometer was located in the reciprocal one, see Figure 4. To compute the average velocity, the same 43 points adopted in the measurements have been used. Results have been obtained up to 3.5 kHz in narrow frequency steps with 240 frequency points per decade and then averaged into one-third octave bands for comparison with measurements. A higher maximum frequency could not be easily achieved due to the

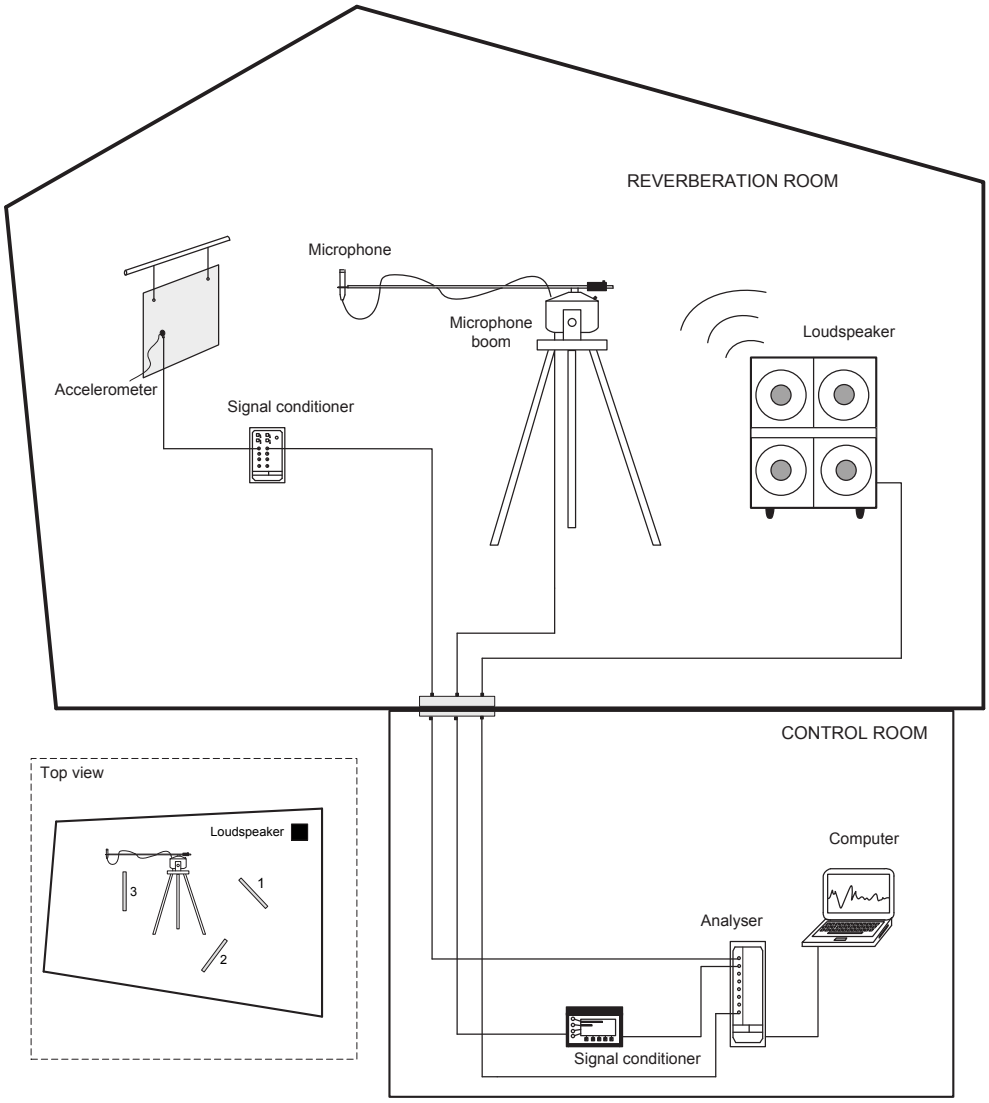

Figure 8: Measurement setup for the reciprocity technique for sound power measurement.

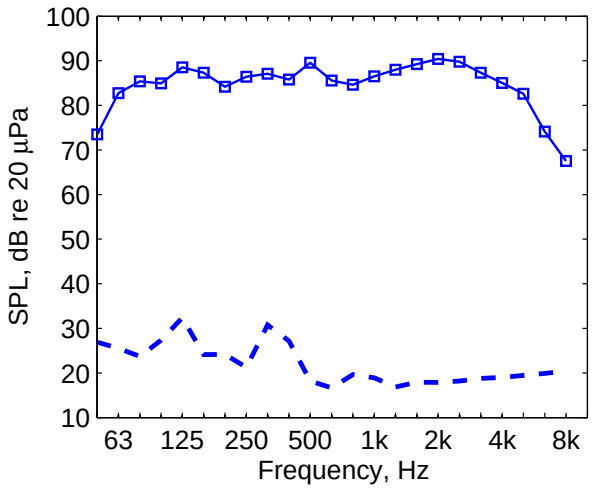

Figure 9: Measured sound pressure level (□) and the noise floor (- - -) inside the reverberation chamber in one-third octave bands.

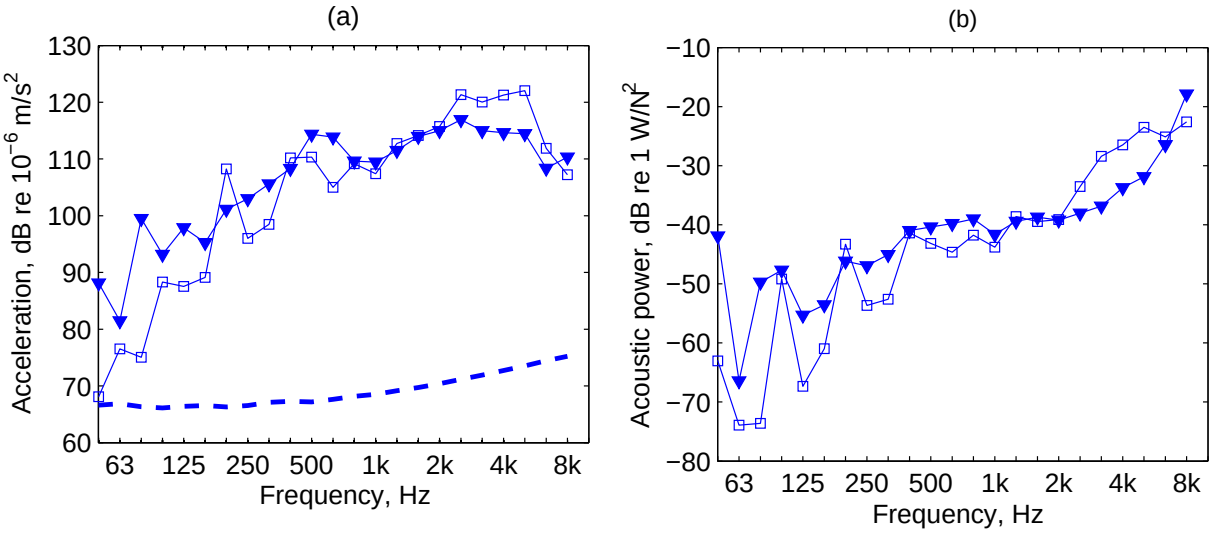

Figure 10: (a) Measured acceleration and (b) radiated sound power in each case from the reciprocity experiment in one-third octave bands: ▾ $t = 1.5$ mm; □ $t = 3$ mm; − − − accelerometer noise floor.

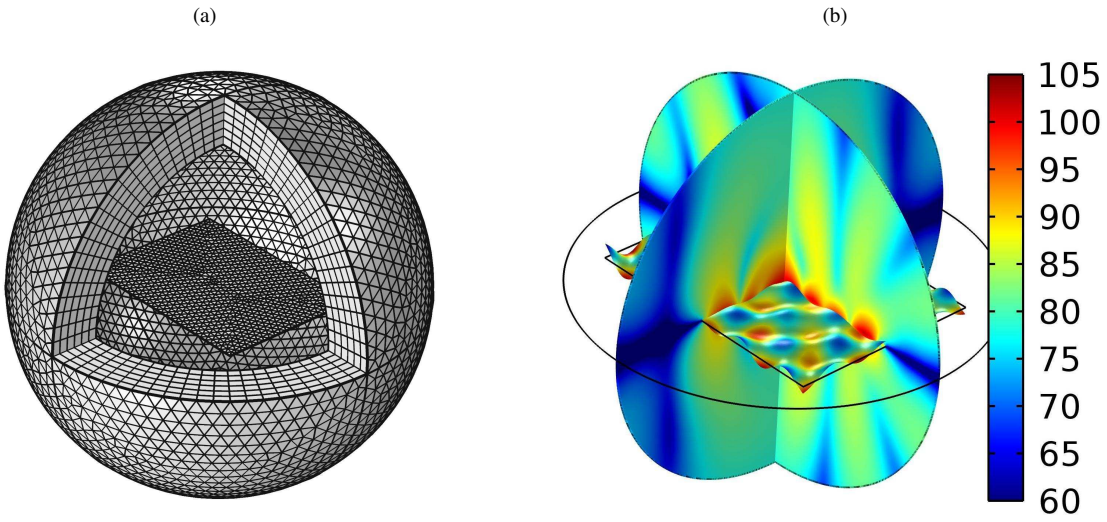

Figure 11: (a) Free plate and Perfect Matching Layer as meshed in COMSOL for the frequency range 2-3 kHz. (b) Example of results calculated at 3 kHz for the 1.5 mm thin plate; the two circular slices represent the sound pressure level (dB re 20 μPa) in the air domain for a unit input force on the plate while the velocity amplitude is depicted on the plate surface; the colourbar refers to the sound pressure level only.

increasing computational time required. The PML is not meant to absorb evanescent waves and this poses a limitation at lower frequency. In this case, with a volume of air enclosed in a sphere of radius 0.3 m and a PML consisting of six layers of elements over a thickness of 0.1 m, the lowest reliable centre frequency has been found to be 200 Hz. There are in fact problems related to the lower frequencies, where the PML becomes less effective due to the presence of evanescent waves, that results in a negative acoustic power. Nevertheless, results are also presented below 200 Hz as the total power was only found to be negative for a small number of frequency points below 180 Hz. As an example Figure 11(a) shows the meshed plate and the PML, while Figure 11(b) shows the sound pressure level in the air domain at 3 kHz for the 1.5 mm thick plate. The velocity amplitude at the same frequency is also plotted over the plate surface.

Figure 12 shows the acoustic power and radiation efficiency in narrow band resolution as calculated using COMSOL and measured with the reciprocal method in the range 100-4000 Hz. The narrow band resolution allows the contribution of single plate modes to be appreciated. This shows up as peaks in the acoustic power and peaks and dips in the radiation efficiency. Very good agreement is found between measurements and modelling. Note that a narrow band resolution of the direct measurement method could not be obtained as the analyser available with the intensity probe only produces results in a few predefined sets of frequency bands, such as one-third, 1/12 or 1/24 octaves. The direct method will be compared with the other two results in the next section.

4.5. Radiation efficiency results

Figure 13 presents the radiation efficiency measured using both the direct and reciprocity techniques along with the numerical results. In general, these show the typical trend expected for the radiation efficiency, with low values at low frequency, increasing towards the critical frequency. For the reciprocity method, the radiation efficiency is obtained by averaging the sound power from the three plate locations in the chamber.

For both plates there is a very good agreement between the reciprocity measurements and the numerical model. An even better agreement could be obtained for the 1.5 mm plate by introducing a frequency-dependent damping in the model. Above 2000 Hz the numerical results are slightly lower than the measurements, which is likely to be due to the chosen loss factor of 0.012 being too low in this range. The direct method, although giving results that are close, shows a slightly different trend. However it has been shown in Section 4.1 that the coupling to the shaker has moved the peaks and modified the apparent damping of the response. In terms of radiated sound power this means that the intensity scan is effectively measuring the sound radiation from a structure which is not behaving exactly the same as when it was freely suspended in the chamber, due to the coupling with the shaker itself. The mode shapes, of course,

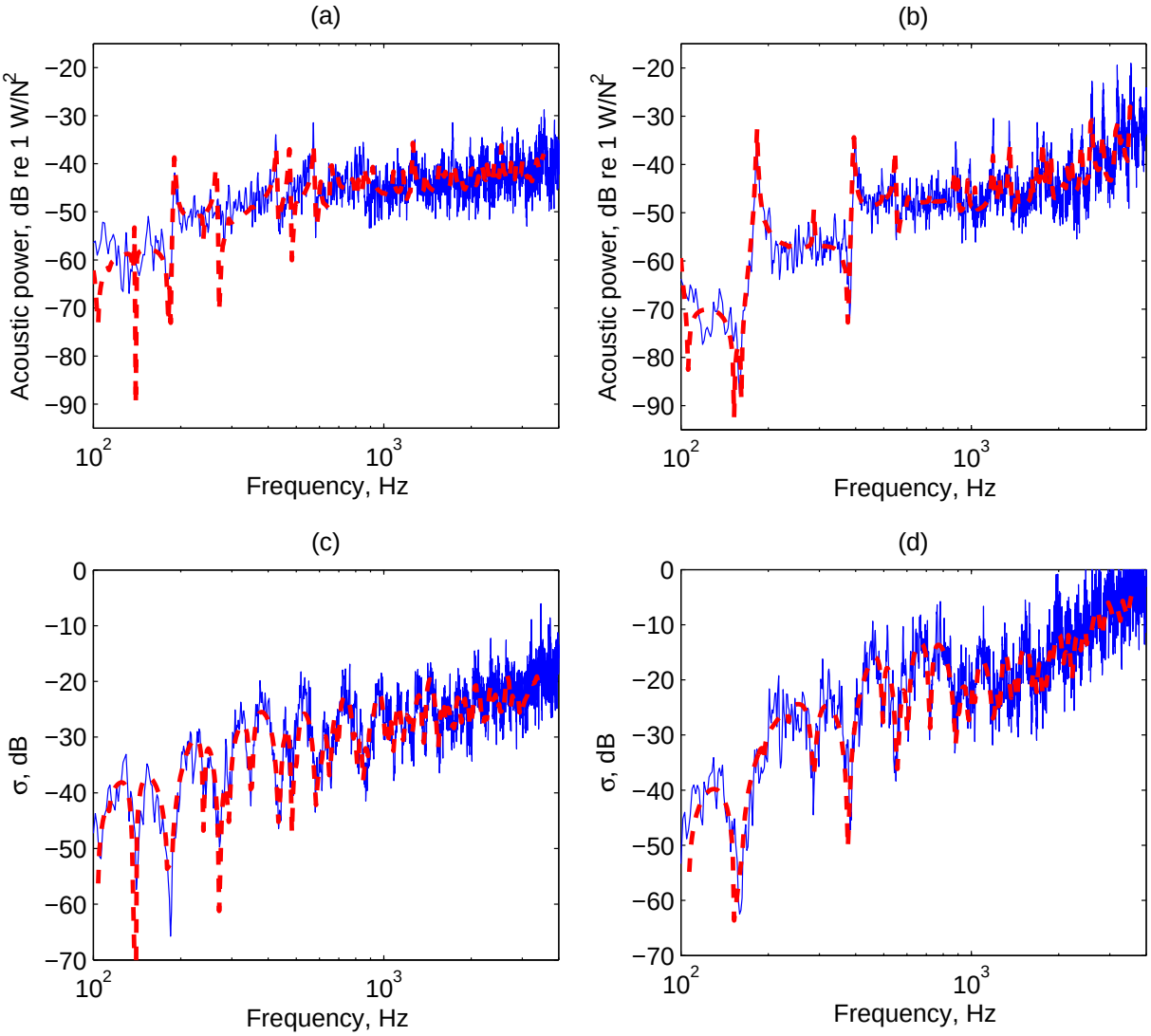

Figure 12: Comparison of narrow band results: — FE model, - - - reciprocal measurement method. (a) Acoustic power for the 1.5 mm plate; (b) acoustic power for the 3 mm plate; (c) radiation efficiency for the 1.5 mm plate; (d) radiation efficiency for the 3 mm plate.

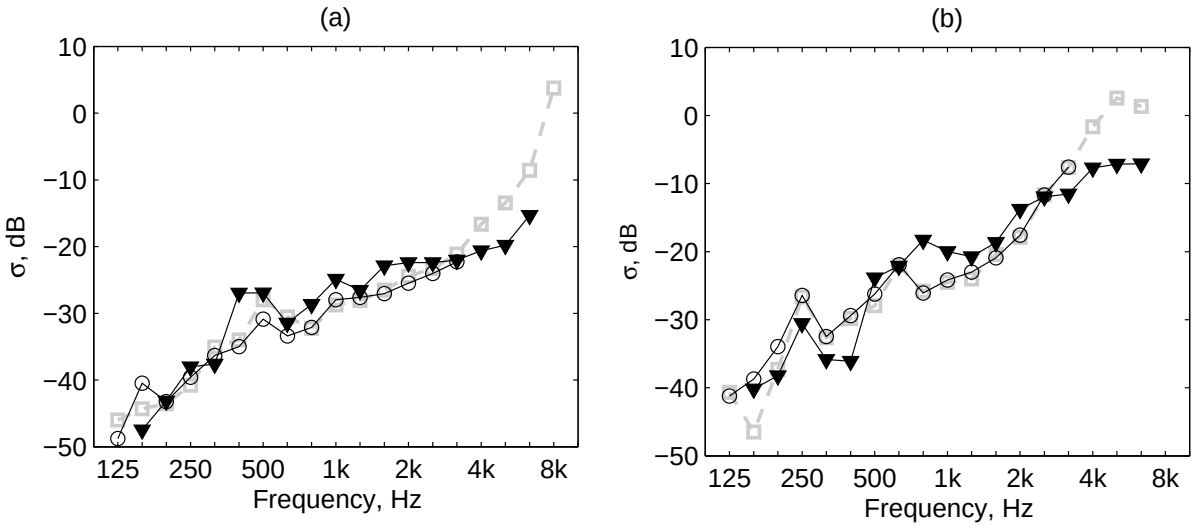

Figure 13: Radiation efficiency results, $10\log_{10}\sigma$, for the free plate; (a) thickness 1.5 mm, (b) thickness 3 mm. —▾—direct method, · · □ · · reciprocity method, –○– FE model.

do not change much but the modes are shifted in frequency and they will combine together in a different way to give a different radiation efficiency. Clearly this depends strongly on the degree of coupling between the shaker and the structure under test. It will be very important for light structures such as the plates examined here while, as will be shown in the next sections, it is less critical for heavier and stiffer structures.

4.6. Effect of force spectrum

A final outcome presented about the radiation efficiency of these plates is related to the effect of the force spectrum. It has been shown in Section 4.1 that the coupling with the shaker results here in increased apparent damping and in moving slightly the position of the peaks in the average velocity of the plate. This effect can be also seen by slightly modifying the postprocessing procedure of the reciprocal method. In this sense Eq. (2) can be rewritten as

$$\sigma = \frac{\overline{a_Q^2}\,\overline{F^2}/\left\langle\overline{p_Q^2}\right\rangle}{\rho c S\left\langle|Y_t|^2\right\rangle\overline{F^2}} \tag{12}$$

which is simply obtained by substituting Eq. (10) in Eq. (2) and then multiplying both numerator and denominator by $\overline{F^2}$. This represents the mean-square force as measured when exciting the plates with the shaker as in the direct method. Clearly, in a narrow band representation of the radiation efficiency, this does not have any effect. However, as the radiation efficiency has been calculated by first representing acoustic power and average velocity (or mobility) in one third octave band and then taking the ratio of the two, the simple operation of Eq. (12) may have a non negligible effect depending on the shape that the force spectrum assumes in a direct measurements. As an example Figure 14 shows the mean-square value of the force measured while exciting the 3 mm plate with the shaker. The presence of the peaks and dips, along with their amplitude, is the reason for the shifted peaks and the increased apparent damping in the average velocity of the direct method: the force has a dip at the plate resonances and a peak at the resonances of the coupled structure leading to peaks in the velocity occurring at these coupled resonances. The change in the bandwidth of the resonances is associated with the forcing function, so this is referred to here as apparent damping. It can be also noted that the natural frequencies of the coupled system are, in the frequency range analysed, always shifted downwards. The reason for this is related to the shaker behaviour that, according to its technical documentation, has its natural frequency at about 50 Hz. Therefore in the coupled system, above 100 Hz, the shaker looks like a mass and moves the natural frequencies downwards with respect to the plate alone.

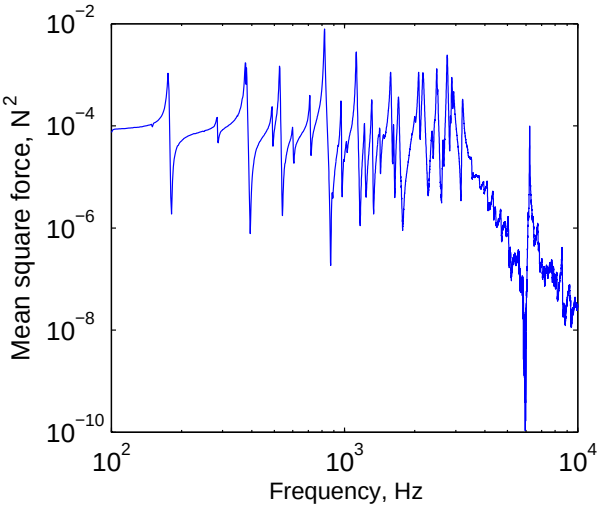

Figure 14: Mean-square force measured while exciting the 3 mm plate with the shaker.

Finally Figure 15 summarises again the radiation efficiencies for both plates. In this case the line representing the reciprocal method has been obtained from Eq. (12), while the direct one is the same as in Figure 13. The reciprocal measurements are now in good agreement with the direct ones up to 2 kHz, confirming that the discrepancies observed in this range in Figure 13 are due to the effect of force spectrum. However this comparison also brings into question the outcomes of the direct method, as applied in this work, for higher frequencies. Although in principle the intensity probe adopted is meant to measure up to 6 kHz, the radiation is clearly underestimated above 2 kHz. There are a number of possible reasons for this result: the lower excitation levels reached in the plates possibly due to stinger misalignment, effects due to imprecision in scanning speed and misalignments of the probe with respect to the normal of the plate surface, effects due to directivity of sound radiated at a grazing angle from the plate that is not measured when scanning over the front face only. Finally, a possible error due to phase mismatch between microphones could also not be completely excluded. However, the actual reasons in the present case have not been identified.

5. Scale model of railway track: measurements and models of rail and sleeper

In this section two further structures are considered. These are components of a 1/5 scale model railway track facility, specifically a 2 m length of rail and a concrete sleeper which is 0.5 m long [24]. The rails are commercially available steel rails used for miniature railways and are approximately 1/5 scale replicas of a UIC 60 section. The concrete sleepers have been specially constructed. A constrained layer damping treatment has been applied to the bottom of the rail foot in order to make the damping of the scaled rail more realistic and to simplify testing. Overall, the damping treatment has increased the damping loss factor to an average value of around 0.026.

The rail and the sleeper have been suspended freely and their radiation has been measured reciprocally in the reverberation chamber. Direct measurements have also been made by forcing the components via a shaker and measuring the sound power with an intensity probe.

The procedures followed to obtain the radiation efficiency are the two already descried in Sections 4.2 and 4.3 with the only difference being that the average mobility measured with an impact hammer has been used for both direct and reciprocal methods and Eq. (2) has been applied. To measure average mobility 41 points equally spaced along the rail have been used, while 11 points have been adopted on the sleeper. In both these cases it has been also verified that coupling with the shaker has less effect than the thin plates. By analysing the force spectrum, average mobility and velocity the same features described in Section 4.1 and 4.6 could be noticed but they are less strong and are not shown here. As the noise radiated from the rail and the sleeper is lower than for the plate, the noise from the shaker becomes more critical. For this reason, in both cases a virtual box has been defined around the objects and the

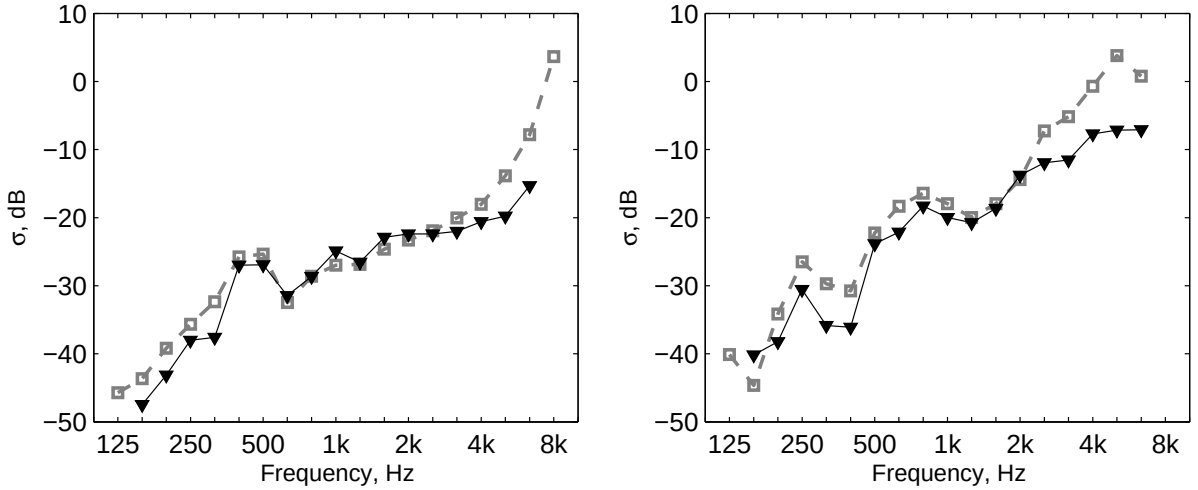

Figure 15: Radiation efficiency results for the free plate; (a) thickness 1.5 mm, (b) thickness 3 mm. —▾—direct method, · · □ · · reciprocity method with modified postprocessing to account for force spectrum measured with the direct technique.

six surfaces enclosing the volume have been scanned according to ISO 9614-3:2002 [3]. Moreover the noise from the shaker has been reduced by locating it in an enclosure, the interior of which was lined with foam.

For both structures an acoustic boundary element model has also been developed using bespoke software for comparison with the two different measurements. In the boundary element model the rail is considered as a two-dimensional rigid body, so the results are obtained for a unit vertical velocity amplitude over the whole section. For this reason any fluctuations in the radiation efficiency due to vibration modes cannot be predicted by the model. For structural wavelengths in the rail greater than the wavelength in air the two-dimensional assumption provides a good approximation. The validity of the two-dimensional approach has been considered in [31] and shown to be valid except at low frequencies. For the scale rail, the critical frequency is found to be at around 300 Hz, below which acoustic short-circuiting occurs. The two-dimensional approach is expected to be valid well above this frequency. For the sleeper, which is shorter, the discrete bending resonances are important so its vibration is modelled as a free-free beam and its sound radiation is modelled using full three-dimensional boundary element model.

Some representations of the measurement set-up are shown in Figure 16, where both direct and reciprocal arrangements are presented for the rail and for the sleeper.

Figure 17(a) shows the radiation efficiency in one-third octave bands for the rail. As can be seen, the radiation efficiency of the rail in free space is proportional to f^3 at low frequency, which is characteristic of a line dipole [31]. The direct method only gave valid results above 700 Hz (800 Hz centre frequency). Below this frequency, the measured acoustic power has consistently been found to be negative which suggests that the noise radiated from the rail is too low compared with the noise radiated from the shaker and with environmental noise. However, between 800 Hz and 4 kHz, the comparison among the three methods is very good.

Figure 17(b) summarises the results obtained on the sleeper. There is a very good agreement between the boundary element model and the measurements performed in the reverberation chamber up to 2 kHz. In this same range the direct measurements show some points in disagreement up to 800 Hz, yet the overall shape is still captured in this range, while they agree better with the other curves between 800 Hz and 2 kHz. An interesting result is found at 500 Hz, where all the methods have detected a clear dip in the radiation efficiency corresponding to the first bending mode of the sleeper. In the next frequency band (630 Hz) the result from the direct method drops further while the reciprocal method and the model both increase together. It has been observed, while analysing results from the direct method, that in this range the sound powers measured on the two opposite faces corresponding to the top and the bottom of the sleeper have different signs, suggesting that the noise coming from outside the virtual box enclosing the sleeper is significant and makes the measurements more difficult and less reliable.

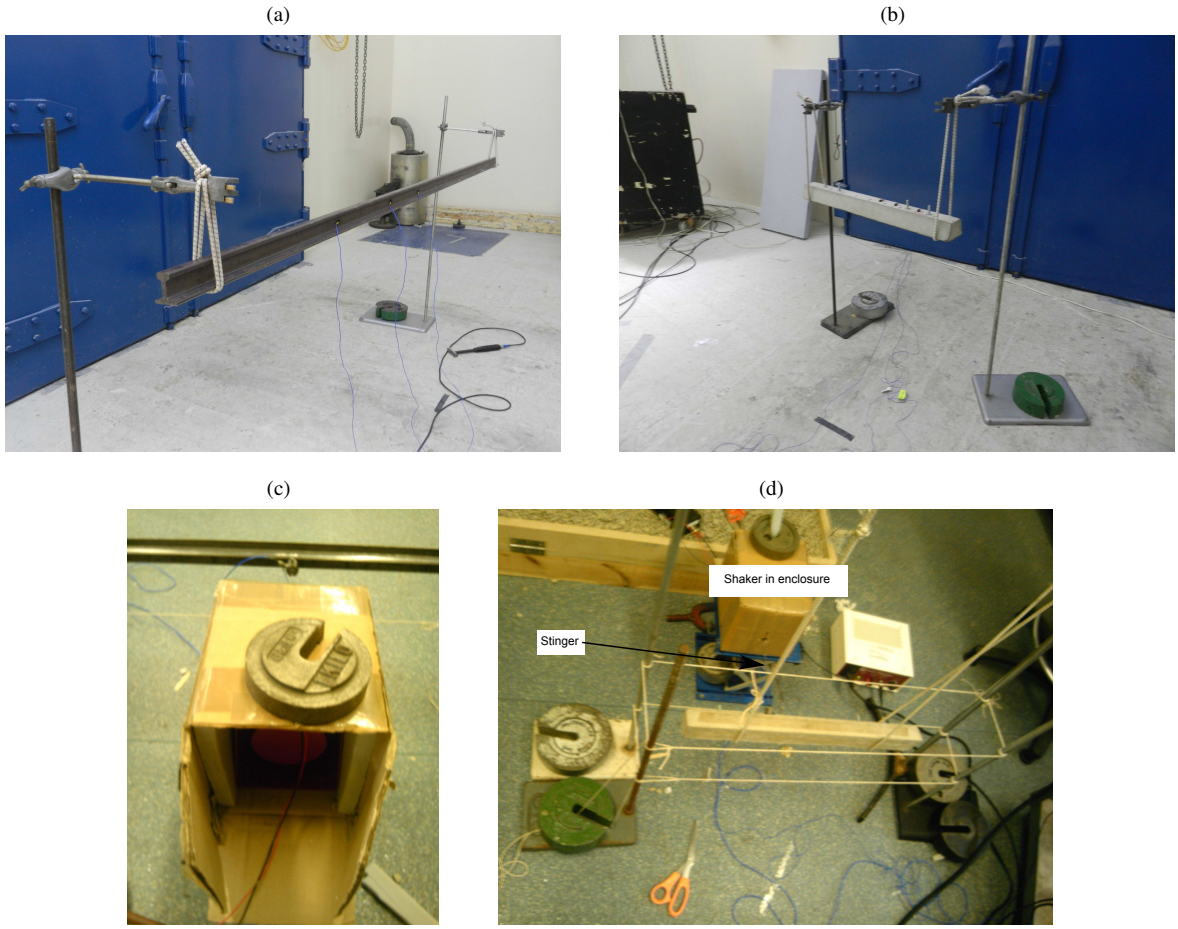

Figure 16: (a) Arrangement for rail radiation efficiency reciprocal measurement in the reverberant room. (b) Arrangement for sleeper radiation efficiency reciprocal measurement in the reverberant room. (c) Arrangement for rail radiation efficiency direct measurement in a general purpose laboratory. (d) Arrangement for sleeper radiation efficiency direct measurement in a general purpose laboratory.

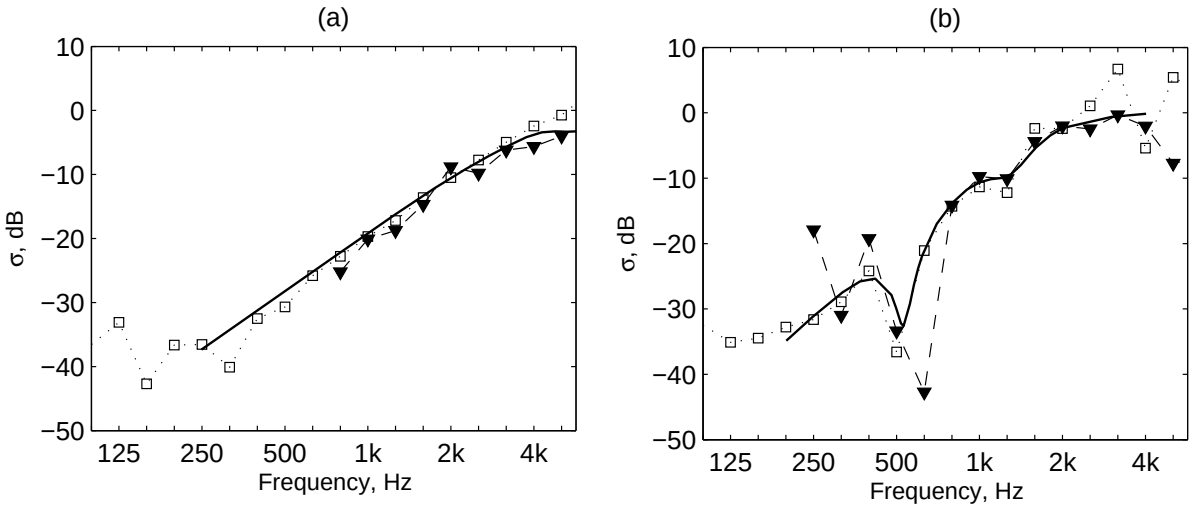

Figure 17: Radiation efficiency results for the free plate; (a) scale model of a rail, (b) scale model of a railway sleeper. —▾— direct method, · · □ · · reciprocity method, — BE model.

Overall, therefore, the measurements on the rail and sleeper show good agreement between the methods and the numerical predictions, although there are some problems associated with the direct method at low frequencies. The shaker connection did not present the same difficulty as for the thin plates.

6. Built-up structures

In order to test the reciprocal method for more complex structures, measurements are finally presented for three built-up structures. These are closed steel box sections 2.67 m long, 0.49 m wide, with heights between 0.37 m and 0.63 m and various different plate thicknesses between 3 and 16 mm (see Figure 18). For each of these box structures the sound power normalised by the mean-square input force has been measured using a direct method as well as the proposed reciprocal method. In the direct method the structures were excited using a small shaker. Both direct and reciprocal methods were performed in the reverberation chamber, therefore without adopting the sound intensity meter. The noise from the shaker was neglible compared with these rather large box structures. In both cases the measurements covered the frequency range 400 to 5000 Hz in one-third octave bands. No prediction model is available in this case but the results are included as an example of more complex structures that can be of interest in practice.

Figure 19 shows the results in terms of radiated power normalised by the input force. In each case the agreement between the two methods is very good. Although there are isolated frequency points with differences of up to 5 dB, the average difference is less than 1 dB for each structure.

In this case the analysis is limited to sound power only as average velocity (or mobility) is not available in sufficient detail and the radiation efficiency has therefore not been estimated. It may be noted that, to assess the radiation efficiency of such a built-up structure, the choice and number of measurement points for the velocity is even more critical than in the case of the homogeneous plate discussed in Appendix A. Stiffening elements cause the vibration levels to be uneven across the vibrating surfaces which makes the definition of the appropriate value for the spatially-averaged mean-square velocity more critical.

7. Conclusions

A reciprocity technique employed in a diffuse field environment has been successfully used to measure the radiation efficiency of several types of structure and the results have been compared with more conventional direct

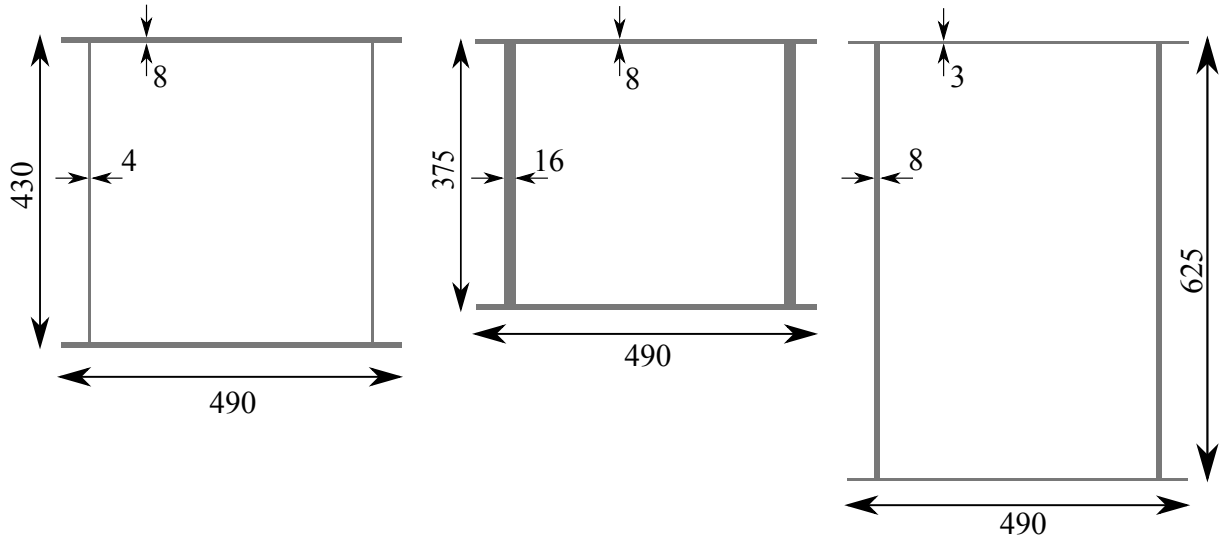

Figure 18: Steel boxes made of welded steel plates and 2.67 m long. From left to right: section A, B and C. Dimensions in mm.

approaches and with numerical models.

First the case of flat rectangular plates has been tested. A very good agreement has been found between the reciprocal method and the numerical models while some differences have been found and discussed in the case of direct measurements. It has been found that for a light structure the coupling with the shaker can be very important and can affect both the structural vibration and the sound radiation and hence the radiation efficiency.

A similar procedure has been applied to test the radiation efficiency of a scale model of a rail and of a sleeper showing a good agreement among the results. Finally three built-up structures have been considered and the reciprocal method has been compared with direct measurements in the reverberation chamber. In this latter case only the sound power measurement has been discussed.

In general it has been found that in applying the reciprocal method in the reverberation chamber it must be ensured that the acoustic excitation is large enough to ensure vibration response levels that are sufficiently greater than the noise floor of the accelerometer. The reciprocal measurement set-up has been shown to be simpler and more flexible compared with the direct approach and is capable of achieving good results over a wider frequency range. In the authors' experience, in the same amount of time more configurations can be tested using the reciprocal method in the reverberation chamber than by adopting a direct method with an intensity probe. The intensity method is, moreover, more sensitive to the external noise and this makes this measurement particularly difficult and unreliable in the range where the structure radiation is low. Applying the direct method in the reverberation chamber can also be a good solution but the noise radiated from the shaker has to be much lower than the noise radiated from the structure to obtain good results. On the other hand the reciprocal method relies on a perfect diffuse field being developed in the chamber and this makes the method less applicable in the low frequency range (typically below 200-300 Hz).

Measuring the radiation efficiency of a vibrating structure is a difficult task. It relies on the ratio of two measured quantities, each of them characterised by measurement uncertainty. The measurement errors present in both numerator and denominator combine to give the error in the measured radiation efficiency. For what concerns the measurements of structural mobility (or direct measurement of velocity) there are issues related to the choice of response and forcing points. To minimise this effect, in the present comparisons the number and location of measuring points has been kept the same in the two measurement methods and, when possible, in the numerical models.

Finally, it has been shown that, for a resonant structure, the shape of the force spectrum affects the radiation efficiency so that care will be required to ensure that result is normalised to an excitation that is representative of the intended application. In particular, the coupling with the shaker in the direct method is shown to modify the radiation efficiency.

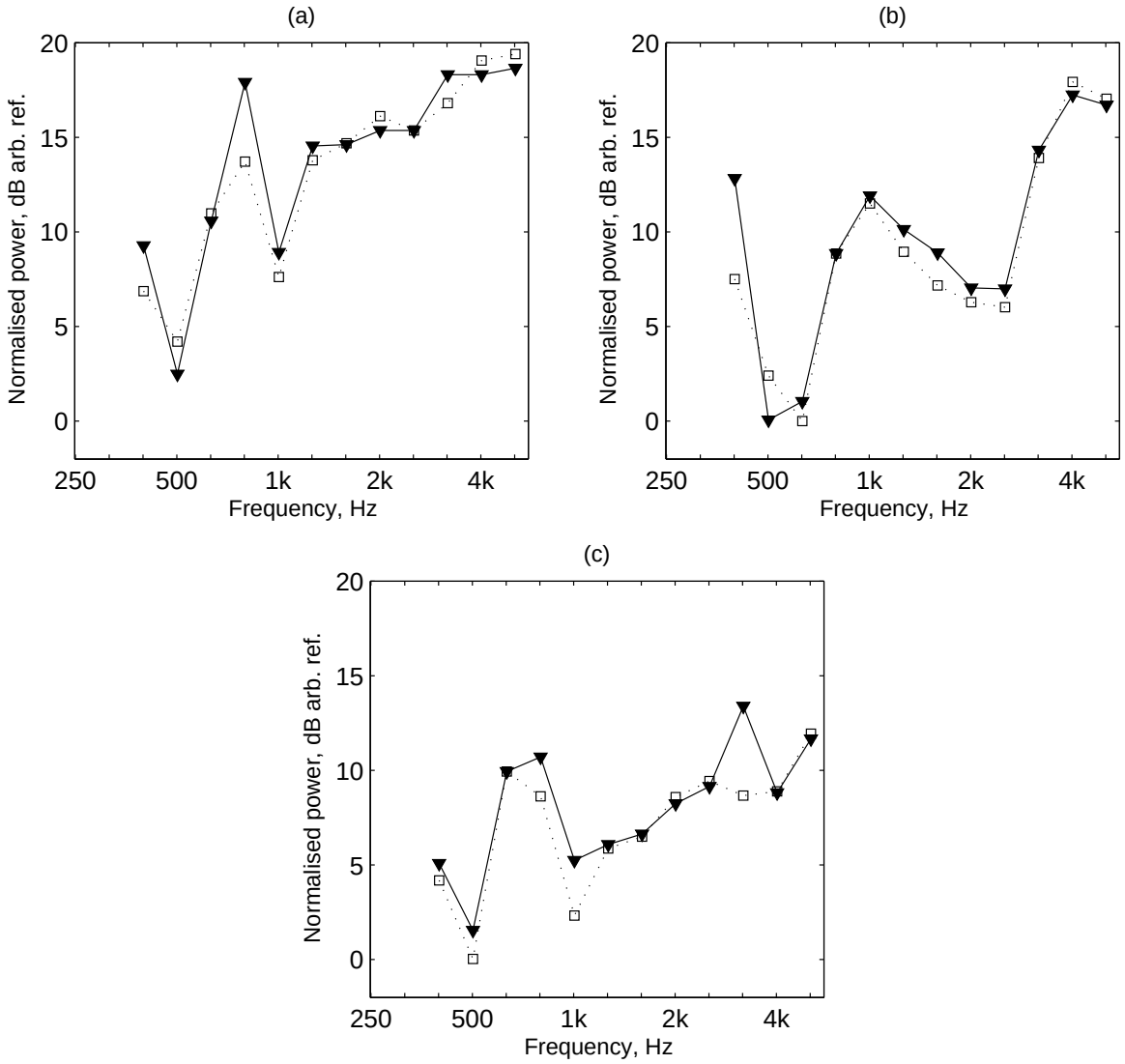

Figure 19: Normalised power for the steel boxes; (a) section A, (b) section B, (c) section C. ▾: direct method; · · □ · · reciprocal method.

Acknowledgements

The reciprocal method was first used by the third author when he was at TNO, the Netherlands, and the measurement results for the built-up structures were obtained there. The authors are grateful to Michael Dittrich of TNO for access to these results. The ideas and inspiration of Prof. Jan Verheij, formlerly of TNO, in developing the method are gratefully acknowledged.

Part of the work presented here has been supported by EPSRC under the programme grant EP/H044949/1, 'Railway Track for the 21st Century'.

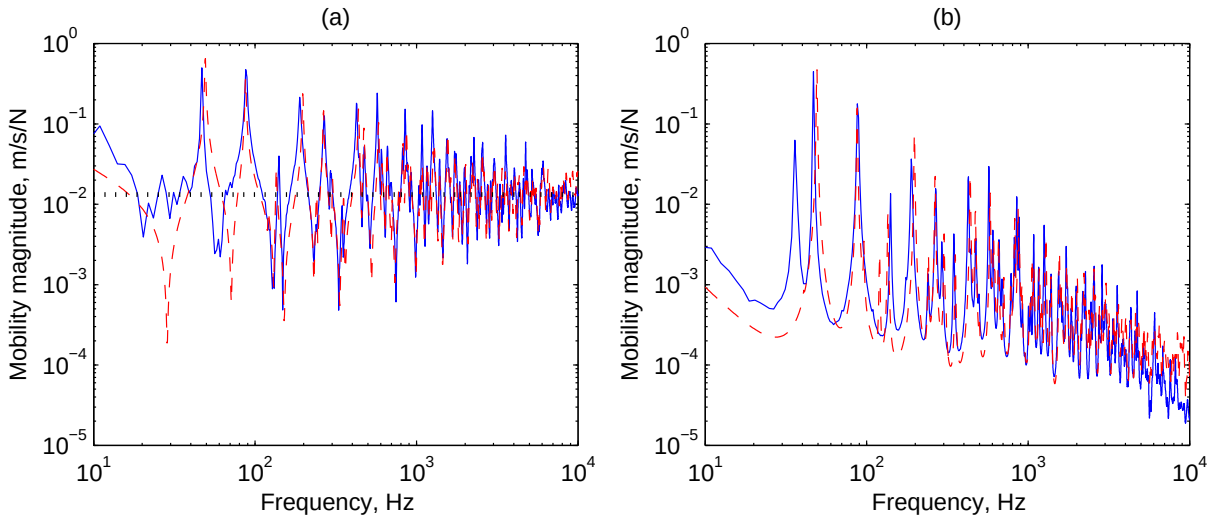

Figure A.1: (a) Driving point mobility and (b) average mobility. — measurements; - - - analytical model; · · · · · · infinite plate.

A. Effect of location of measurement point for a freely suspended plate

This appendix shows the effect that the number and location of measurements points over a flat plate has on the estimation of spatially-averaged mobility. The plate considered as an example is one of the two aluminium plates considered in the paper having surface dimensions of 0.4 m× 0.3 m and thickness of 1.5 mm. The average mobility has been calculated for various measurement grids with the force always located at the same point (the driving point A of Figure 4). Here, an analytical model for forced vibrations of a free plate has been adopted. The model is based on the approximate vibration modes solution given by Warburton [32] and the mobility has been calculated by modal superposition as:

$$Y_t(x,y,x_0,y_0) = \sum_{m=0}^{\infty}\sum_{n=0}^{\infty} \frac{j\omega\phi_{mn}(x_0,y_0)\phi_{mn}(x,y)}{[\omega_{mn}^2(1+j\eta)-\omega^2]M_{mn}} \tag{A.1}$$

where ϕ_{mn} indicates mode shape, ω_{mn} the natural frequency and M_{mn} the modal mass of the vibration mode (m,n). x_0 and y_0 represent the coordinates of the forcing point while x and y represent any point on the plate where the mobility is calculated.

The modal loss factor η has been set equal to 0.012 and for simplicity is kept the same for all the vibration modes.

Figure A.1 shows the driving point mobility and average mobility as measured with the impact hammer test and as estimated with the analytical model. The average mobility shown in the figure is based on the measurement grid of Figure 4. Although there is not a perfect correspondence between measurements and model it can be seen that the model is accurate enough for a parametric investigation on the effect the measurement grid. In Figure A.1, with the aim of verifying the analytical model against measurements, all the modes with natural frequency up to 10 kHz have been included in the double summation of Eq. (A.1), while the subsequent parametric analysis on the grid effect has been performed in a frequency range between 0 and 5 kHz. In this case the double summation includes all the modes up to 6 kHz.

The average mobility has been calculated for an increasing number of measurements points on the plate starting from 1 up to 300, for a total of 50 configurations. These are defined with a linear spacing between 10 and 300 and ten more configurations between 1 and 10 measurement points. For each configuration the measurement points have been randomly located on the plate. The average mobility corresponding to each configuration has been converted into one-third octave bands resulting in a lowest centre frequency of 12.5 Hz and highest of 4 kHz. The configuration with 300 points is used as a reference and the difference between each configuration and this have been determined

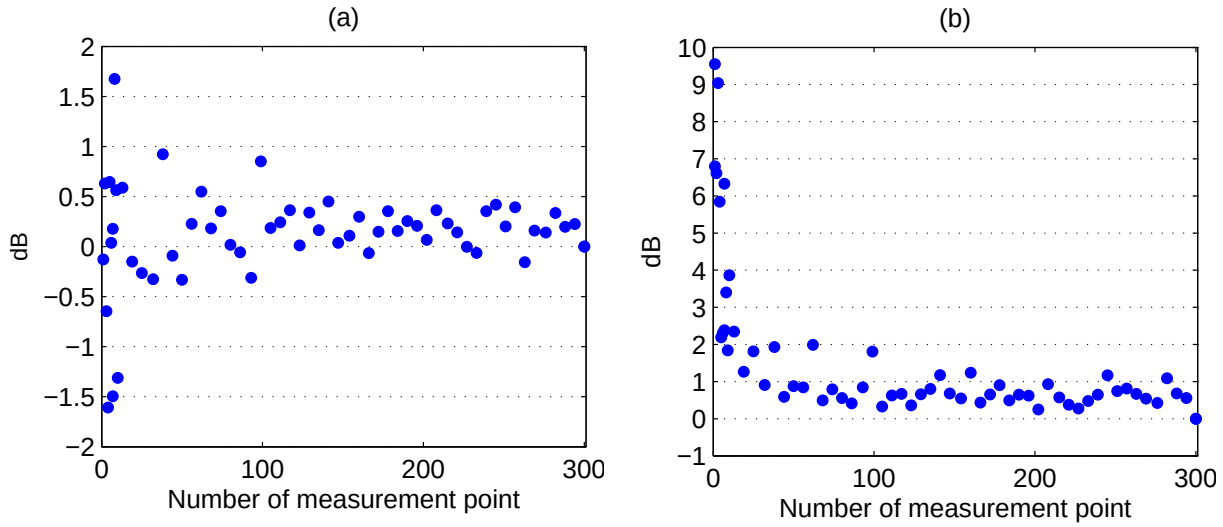

Figure A.2: Each point in the figure represents (a) the average or (b) the maximum difference in one-third octave bands (centre frequency range: 12.5-4000 Hz) between the spatially-averaged mobility of each configuration and the results obtained on the grid consisting of 300 points.

in each frequency band. The average difference over all frequency bands and the maximum difference in a frequency band are identified for each configuration. Figure A.2 shows these results for the increasing number of measurements points. Clearly the average difference decreases but it is interesting to observe that the relative difference between two adjacent configurations can be significant even with more than 50 measurement points and it is necessary to have more than 100 measurement points for the average mobility variation to be always less than $\pm$ 0.5 dB. The maximum difference is never found to be consistently lower than 1 dB. Note that these outcomes depend on the particular random selections. Nevertheless they give a clear idea of the overall trend of this effect.

For the reasons outlined above, all the structural vibration tests on the two plates have been performed on exactly the same grid so as to avoid unwanted variability among the results.

[1] Acoustics - Determination of sound power levels and sound energy levels of noise sources using sound pressure precision method for anechoic rooms and hemi-anechoic rooms (ISO 3745:2012), International Standard Organisation.
[2] Acoustics - Determination of sound power levels and sound energy levels of noise sources using sound pressure precision methods for reverberation test rooms (ISO 3741:2010), International Standard Organisation.
[3] Acoustics - Determination of sound power levels of noise sources using sound intensity - Part 3: Precision method for measurement by scanning (ISO 9614-3:2002), International Standard Organisation.
[4] J. R. Wright, G. W. Skingle, On the direct or indirect measurement of force in vibration testing, in: 15th International Modal Analysis Conference, Society of Photo-Optical Instrumentation Engineers, 1997.
[5] McConnell, P. Cappa, Transducer inertia and stinger stiffness effect on FRF measurements, Mechanical Systems and Signal Processing 14 (4) (2000) 625–636.
[6] J. W. Strutt Rayleigh, The Theory of Sound, 2nd Edition, Dover, 1945.
[7] F. Fahy, P. Gardonio, Sound and structural vibration radiation, transmission and response (2007).
[8] L. M. Lyamshev, A method for solving the problem of sound radiation by thin elastic shells and plates, Soviet Physics Acoustics 5 (1959) 122–124.
[9] L. M. Lyamshev, A question in connection with the principle of reciprocity in acoustics, Soviet Physics Doklady 4 (1959) 406.
[10] F. J. Fahy, The vibro-acoustic reciprocity principle and applications to noise control, Acta Acustica united with Acustica (1995) 544–558.
[11] F. J. Fahy, Some applications of the reciprocity principle in experimental vibroacoustics, Acoustical Physics 49 (2) (2003) 217–229.
[12] J. W. Verheij, Inverse and reciprocity methods for machinery noise source characterization and sound path quantification. Part 1: sources, International Journal of Acoustics and Vibration 2 (1997) 11–20.
[13] J. W. Verheij, Inverse and reciprocity methods for machinery noise source characterization and sound path quantification. Part 2: transmission paths, International Journal of Acoustics and Vibration 2 (1997) 103–112.
[14] J. Zheng, F. Fahy, D. Anderton, Application of a vibro-acoustic reciprocity technique to the prediction of sound radiated by a motored IC engine, Applied Acoustics 42 (4) (1994) 333–346.
[15] G. J. Kim, K. R. Holland, N. Lalor, Identification of the airborne component of tyre-induced vehicle interior noise, Applied Acoustics 51 (2) (1997) 141–156.
[16] B. S. Kim, G. J. Kim, T. K. Lee, The identification of tyre induced vehicle interior noise, Applied Acoustics 68 (1) (2007) 134–156.
[17] J. M. Mason, F. Fahy, Development of a reciprocity technique for the prediction of propeller noise transmission through aircraft fuselages, Engineering Noise Control Journal 34 (1990) 43–51.
[18] D. G. MacMartin, G. L. Basso, F. W. Slingerland, Aircraft fuselage noise transmission measurements using a reciprocity technique, Journal of Sound and Vibration 187 (3) (1995) 467–483.
[19] J. D. Maynard, E. G. Williams, Y. Lee, Nearfield acoustic holography: I. Theory of generalized holography and the development of NAH, The Journal of the Acoustical Society of America 78 (4) (1985) 1395–1413.
[20] M. Villot, G. Chavériat, J. Roland, Phonoscopy: An acoustical holography technique for plane structures radiating in enclosed spaces, The Journal of the Acoustical Society of America 91 (1) (1992) 187–195.
[21] M. J. Crocker, A. J. Price, Sound transmission using statistical energy analysis, Journal of Sound and Vibration 9 (3) (1969) 469–486.
[22] A. Elmallawany, Calculation of sound insulation of ribbed panels using statistical energy analysis, Applied Acoustics 18 (4) (1985) 271–281.
[23] R. Zhou, M. J. Crocker, Sound transmission loss of foam-filled honeycomb sandwich panels using statistical energy analysis and theoretical and measured dynamic properties, Journal of Sound and Vibration 329 (6) (2010) 673–686.
[24] X. Y. Zhang, D. J. Thompson, G. Squicciarini, Influence of ground impedance on the sound radiation of a railway track, in: Proceedings of 21st International Congress on Sound and Vibration, Beijing, China, 2014.
[25] F. Fahy, Foundations of Engineering Acoustics, 1st Edition, Academic Press, 2000.
[26] L. E. Kinsler, A. R. Frey, A. B. Coppens, J. V. Sanders, Fundamentals of Acoustics, 4th Edition, Wiley, 1999.
[27] E. Skudrzyk, The meanvalue method of predicting the dynamic response of complex vibrators, The Journal of the Acoustical Society of America 67 (4) (1980) 1105–1135.
[28] M. R. Schroeder, Frequency correlation functions of frequency responses in rooms, The Journal of the Acoustical Society of America 34 (12) (1962) 1819–1823.
[29] Q. Liu, J. Tao, The perfectly matched layer for acoustic waves in absorptive media, The Journal of the Acoustical Society of America 102 (4) (1997) 2072–2082.
[30] M. Zampolli, N. Malm, A. Tesei, Improved perfectly matched layers for acoustic radiation and scattering problems, in: Proceedings of the COMSOL conference, 2008.
[31] D. J. Thompson, C. J. C. Jones, N. Turner, Investigation into the validity of two-dimensional models for sound radiation from waves in rails, The Journal of the Acoustical Society of America 113 (4) (2003) 1965–1974.
[32] G. B. Warburton, The Vibration of Rectangular Plates, Proceedings of the Institution of Mechanical Engineers 168 (1) (1954) 371–384.